LETTER

doi:10.1038/nature12020

Anomalous sulphur isotopes in plume lavas reveal deep mantle storage of Archaean crust

Rita A. Cabral[1], Matthew G. Jackson[1], Estelle F. Rose-Koga[2], Kenneth T. Koga[2], Martin J. Whitehouse[3,4], Michael A. Antonelli[5], James Farquhar[5], James M. D. Day[6] & Erik H. Hauri[7]

Basaltic lavas erupted at some oceanic intraplate hotspot volcanoes are thought to sample ancient subducted crustal materials[1,2]. However, the residence time of these subducted materials in the mantle is uncertain and model-dependent[3], and compelling evidence for their return to the surface in regions of mantle upwelling beneath hotspots is lacking. Here we report anomalous sulphur isotope signatures indicating mass-independent fractionation (MIF) in olivine-hosted sulphides from 20-million-year-old ocean island basalts from Mangaia, Cook Islands (Polynesia), which have been suggested to sample recycled oceanic crust[3,4]. Terrestrial MIF sulphur isotope signatures (in which the amount of fractionation does not scale in proportion with the difference in the masses of the isotopes) were generated exclusively through atmospheric photochemical reactions until about 2.45 billion years ago[5–7]. Therefore, the discovery of MIF sulphur in these young plume lavas suggests that sulphur—probably derived from hydrothermally altered oceanic crust—was subducted into the mantle before 2.45 billion years ago and recycled into the mantle source of Mangaia lavas. These new data provide evidence for ancient materials, with negative $\Delta^{33}S$ values, in the mantle source for Mangaia lavas. Our data also complement evidence for recycling of the sulphur content of ancient sedimentary materials to the subcontinental lithospheric mantle that has been identified in diamond-hosted sulphide inclusions[8,9]. This Archaean age for recycled oceanic crust also provides key constraints on the length of time that subducted crustal material can survive in the mantle, and on the timescales of mantle convection from subduction to upwelling beneath hotspots.

Oceanic crust and sediments are introduced to the mantle at subduction zones, but the fate of this subducted material within the mantle, as well as the antiquity of this process, is unknown. Earth's mantle is chemically and isotopically heterogeneous, and it has been suggested that some of this heterogeneity derives from geochemically diverse subducted oceanic[1] and continental[2] crustal material that is mixed with the ambient mantle following subduction. It has also been suggested that different types of crustal materials generate different isotopic endmembers in the mantle[10]—including HIMU (high $\mu = {}^{238}U/{}^{204}Pb$), EM1 (enriched mantle I) and EM2 (enriched mantle II)—and these endmembers are sampled by mantle melts erupted at oceanic hotspot volcanoes. Owing to the loss of fluid-mobile Pb from altered basalt during subduction[11], oceanic crust processed in subduction zones is thought to form a HIMU reservoir in the mantle and, over time, this reservoir develops extreme radiogenic Pb-isotope compositions[1,3,4,10].

Basaltic lavas on the island of Mangaia exhibit the most radiogenic Pb-isotope compositions observed in ocean island basalt (OIB) globally (see, for example, refs 3 and 4) and represent the HIMU mantle endmember. Mangaia lavas have long been suggested to sample melts of recycled oceanic crust[3,4]. However, such an origin for this signature has been questioned and alternative models that favour metasomatic processes to generate the HIMU mantle beneath Mangaia have been suggested[12,13]. Here we report MIF S-isotope compositions in Mangaia lavas that require the presence of recycled, ancient (>2.45 Gyr old) surface material in the HIMU mantle source for Mangaia lavas.

Fresh basaltic glass for S-isotope measurement is not available from Mangaia, where subaerial lavas are ~20 million years old[14] and have suffered from extensive weathering in a tropical climate. However, magmatic olivine phenocrysts encapsulate primary magmatic sulphides and isolate them from surface weathering processes. Olivine phenocrysts were separated from three basaltic lavas collected from Mangaia. The largest inclusions were exposed for S-isotope analysis by secondary ion mass spectrometry (SIMS). Whereas sulphides <10 μm in diameter are relatively common, the largest sulphides, which permit replicate S-isotope measurements, are exceedingly rare (thousands of olivine fragments from many kilograms of rock were examined individually under a microscope and only two sulphide inclusions were large enough to permit replicate S-isotope analyses). The other sulphides were either too small for measurement by SIMS, or were sufficiently large for only a single S-isotope analysis (see Supplementary Information and Fig. 1 for sulphide descriptions). An olivine separate was prepared and analysed using chemical extraction techniques and gas-source isotope ratio mass spectrometry (IRMS) to provide an independent measurement comparison with the SIMS results.

Sulphur isotopes were measured by SIMS at the NordSIMS facility in Stockholm, Sweden, in four sulphide inclusions recovered from

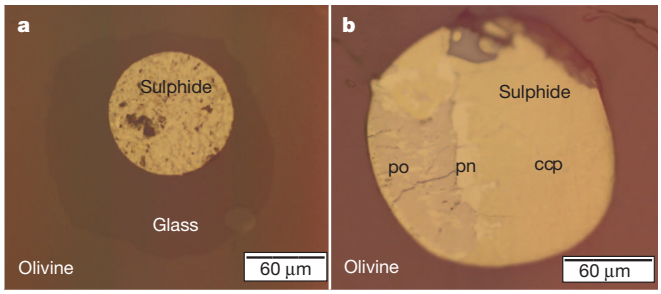

Figure 1 | Reflected-light photomicrographs of sulphide inclusions. **a**, MGA-B-47 sulphide inclusion. The sulphide was homogenized on a heating stage before exposure and analysis, and the primary magmatic sulphide mineralogy was lost during this process. **b**, MGA-B-25 sulphide inclusion. The sulphide was not homogenized, and hosts three coexisting magmatic phases: chalcopyrite (ccp), pentlandite (pn) and pyrrhotite (po). The other two sulphides examined in this study (not shown, see Supplementary Fig. 3) were separated from whole rock sample MG1001. The MG1001B-S17 sulphide inclusion contains chalcopyrite and pyrrhotite. The MG1001B-S14 sulphide inclusion, which does not have a $\Delta^{33}S$ anomaly, contains pyrrhotite, pentlandite, chalcopyrite and pyrite (a low-temperature sulphide phase consistent with a non-magmatic origin).

[1]Department of Earth and Environment, Boston University, 675 Commonwealth Avenue, Boston, Massachusetts 02215, USA. [2]Laboratoire Magmas et Volcans, Université Blaise Pascal, CNRS UMR6524, IRD R163, 5 rue Kessler, 63038 Clermont-Ferrand, France. [3]Swedish Museum of Natural History, Box 50007, SE-104 05 Stockholm, Sweden. [4]Department of Geological Sciences, Stockholm University, SE-106 91 Stockholm, Sweden. [5]Department of Geology and ESSIC, University of Maryland, College Park, Maryland 20742, USA. [6]Geosciences Research Division, Scripps Institution of Oceanography, La Jolla, California 92093-0244, USA. [7]Department of Terrestrial Magnetism, Carnegie Institution of Washington, Washington DC 20015, USA.

three basaltic hand samples. Multiple spot analyses were made on each of the two largest sulphides, MGA-B-25 (ten spot analyses) and MGA-B-47 (nine spot analyses), and a single spot analysis was performed on each of two small sulphide inclusions from MG1001 (sulphides S14 and S17). Individual measurements of MGA-B-25 and MGA-B-47 were averaged (see discussion in Supplementary Information), and give negative $\Delta^{33}S$ anomalies (weighted averages -0.25 ± 0.07‰ (2σ) and -0.34 ± 0.08‰ (2σ), respectively; see Supplementary Information for discussion of uncertainty, and Supplementary Table 3) that are statistically resolvable from ambient mantle sulphur ($\Delta^{33}S = 0$). Here $\Delta^{33}S = \delta^{33}S - [(1 + \delta^{34}S)^{0.515} - 1]$, $\delta^{33}S_{V\text{-}CDT} = [(^{33}S/^{32}S)_{sample}/(^{33}S/^{32}S)_{V\text{-}CDT}] - 1$, and similarly for $\delta^{34}S$ (details of the standards are given in the Supplementary Information). The two sulphide inclusions from sample MG1001 gave overlapping $\Delta^{33}S$ values: inclusions S17 and S14 have respective $\Delta^{33}S$ values of -0.17 ± 0.27‰ (2σ) and 0.03 ± 0.28‰ (2σ). The anomaly-free sulphide phase hosts pyrite, which is consistent with a low-temperature, non-magmatic (modern) origin for the sulphur in this sulphide, and suggests that not all olivine-hosted sulphides in Mangaia lavas are magmatic. The $\delta^{34}S$ values of all sulphide inclusions are less than -6.1‰ (see Supplementary Information for discussion of $\delta^{34}S$ measurements), which are generally more negative than the values encountered previously in magmatic sulphide inclusions[15]. The possibility of dilution with normal mantle S (at $\Delta^{33}S = 0$, $\delta^{34}S = 0$) during the magmatic process means that our inclusion data probably represent mixtures, and more extreme compositions may exist in the low $\delta^{34}S$–negative MIF source region; some evidence for this dilution comes from the apparent 'mixing line' of the inclusions, the bulk olivine and ambient mantle (Fig. 2). Alternatively, the S-isotope trend may simply reflect isotopic diversity observed in melt inclusions from Mangaia[16].

Following sulphur extraction by wet chemistry, S isotopes were also measured in ~400 mg of bulk olivine separates from whole rock sample MGA-B-47 by gas-source IRMS at the University of Maryland. $\Delta^{33}S$ (-0.12 ± 0.04‰) and $\delta^{34}S$ (-3.28 ± 2‰) values are identified in the bulk olivine separate (Supplementary Table 5), but the values are smaller in magnitude than observed in the magmatic sulphides from this sample. We consider it likely that the magnitude of $\Delta^{33}S$ and $\delta^{34}S$ in the bulk olivine separates was diminished relative to the individual magmatic sulphides by incorporation of sulphur into the bulk olivine measurement, either through post-lava flow emplacement of secondary pyrite in Mangaia olivines, or through dilution of an Archaean MIF-S signature by mixing with an ambient mantle S-isotope composition.

Lead-isotope compositions of the two largest inclusions exhibiting the clearest $\Delta^{33}S$ anomalies were also measured by SIMS (Fig. 3; see Methods and Supplementary Information). Both sulphide inclusions exhibit Pb-isotope signatures indistinguishable from the whole rock Pb-isotope analyses[3], confirming that the anomalous S-isotope compositions are associated with the HIMU mantle reservoir. Olivine-hosted sulphide inclusions from this locality were previously found to have endmember HIMU compositions[16,17].

A modern origin of the $\Delta^{33}S$ anomaly in Mangaia sulphides is improbable. Small variations in $\Delta^{33}S$ (from -0.05‰ to $+0.34$‰)

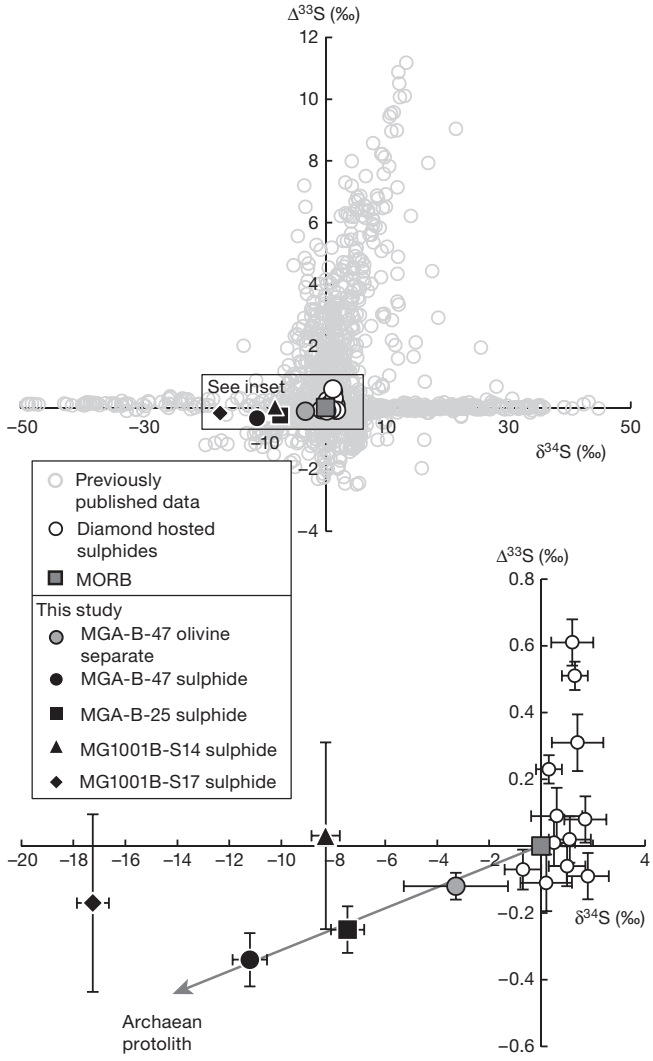

Figure 2 | $\Delta^{33}S$ versus $\delta^{34}S$ for olivine-hosted sulphide inclusions from Mangaia (this study) and diamond-hosted sulphides (from ref. 8) compared to previously published S-isotope data. Points shown are the weighted averages of the individual analyses for MGA-B-47 and MGA-B-25 ($n = 9$ for MGA-B-47; $n = 10$ for MGA-B-25) and single analyses for both MG1001 samples. Error bars are 95% confidence level for the MGA-B-25 and MGA-B-47 weighted averages and 2σ for the single analyses. The isotope composition of the bulk olivine separate is also shown (see Supplementary Information). Previously published sulphur isotope data are after figure 1 in ref. 7.

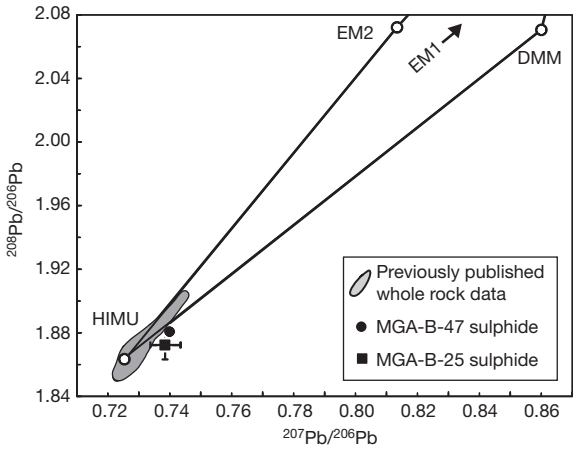

Figure 3 | The Pb-isotope composition of olivine-hosted sulphides are the same as Mangaia whole rocks. The Pb-isotope compositions of the two olivine-hosted sulphides from MGA-B-25 and MGA-B-47 were obtained by SIMS measurement (see Supplementary Information), and whole rock Pb-isotopes for these samples were characterized in ref. 3. The new sulphide data (black symbols) cluster around the HIMU mantle endmember defined by previously published whole rock Pb-isotope data from Mangaia lavas (grey field, using whole rock data from ref. 4 and references therein). The apices of the quadrilateral are defined by the isotopic endmembers found in the oceanic mantle (EM1, EM2, HIMU, DMM (depleted MORB mantle)). The average of two Pb-isotope measurements of the same inclusion are shown for MGA-B-25 (see Supplementary Table 4). Error bars reflect the 2σ standard error of the mean (MGA-B-47) or the 2σ weighted error of the mean (for the two measurements of MGA-B-25).

can be generated by biologically-controlled mass-dependent fractionation mechanisms[18–20], but these mechanisms tend to generate positive $\Delta^{33}S$ values when $\delta^{34}S$ values are negative, and negative $\Delta^{33}S$ when $\delta^{34}S$ values are positive, rather than the observed negative $\Delta^{33}S$ and $\delta^{34}S$ values in Mangaia sulphides. These processes are also only known to generate smaller magnitude negative $\Delta^{33}S$ anomalies than those observed in Mangaia sulphides.

Assimilation of ancient crustal materials is also an unlikely source of the $\Delta^{33}S$ anomalies. The oceanic lithosphere beneath Mangaia is too young to have formed at a time when MIF S is known to have occurred. It is also unlikely that Mangaia lavas were contaminated by stranded blocks of Archaean continental crust, as tectonic reconstructions of the Pacific plate[21] place Mangaia far from the locus of continental rifting and from Pacific fracture zones that may have stranded ancient continental material in this oceanic basin (see, for example, refs 22 and 23).

We suggest that MIF S in Mangaia lavas comes from a mantle reservoir containing S subducted before 2.45 Gyr ago. The subducted S was preserved in the convecting mantle, and remained associated with the subducted package (subducted lithosphere ± sediments), so that its Archaean MIF signature was not completely diluted during its >2.45-Gyr residence in the mantle. The lower mantle may be a 'graveyard' for subducted Archaean crust with negative $\Delta^{33}S$ (ref. 8). Less vigorous convective motions in this part of the mantle may be more conducive to preserving mantle heterogeneities over long timescales. Processes associated with buoyant upwelling could have transported MIF-S-bearing material back to the surface where it melted beneath Mangaia at 20 Myr ago. Sulphides in Mangaia melts were trapped and encapsulated in growing magmatic olivine phenocrysts, thus preserving the MIF signature during magma transport and eruption.

Positive and negative $\Delta^{33}S$ have been documented previously in diamond-hosted sulphide inclusions[8,9], and these data complement the negative $\Delta^{33}S$ measurements reported in Mangaia. A conceptual model suggested (ref. 8) for the origin of the positive $\Delta^{33}S$ signature in the diamond-hosted sulphides sheds light on the possible origins of the negative $\Delta^{33}S$ in Mangaia. Photolysis of volcano-sourced Archaean sulphur (with initial $\Delta^{33}S = 0‰$) occurred in an oxygen-poor (and therefore ozone-poor) atmosphere relatively transparent to solar ultraviolet radiation. Photochemical fractionation acting on atmospheric sulphur species generated geochemical reservoirs with complementary positive $\Delta^{33}S$ (reduced and elemental sulphur species) and negative $\Delta^{33}S$ (oxidized species such as sulphate). Elemental sulphur with positive $\Delta^{33}S$ in the atmosphere was deposited in surface reservoirs and converted to sulphide. The positive $\Delta^{33}S$ of the sulphur identified in the diamond-hosted sulphide inclusions corresponds to that found in Archaean sedimentary sulphides, suggesting a sedimentary origin for the positive $\Delta^{33}S$ in the diamond-hosted sulphides[8]. The Archaean sulphur-bearing sediment was subducted into the mantle source of the Orapa diamonds, encapsulated in diamond, and preserved until transport to the surface in a kimberlite eruption.

The data reported here include the first observation of non-zero $\Delta^{33}S$ in OIB. We suggest that the negative $\Delta^{33}S$ identified in Mangaia sulphides originates from the Archaean oceanic sulphate pool that is complimentary to the sedimentary pyrite, and that this MIF S-isotope signature was incorporated into oceanic crust following bisulphide formation in Archaean hydrothermal systems (Supplementary Fig. 1). Archaean rocks with a clear oceanic association tend to exhibit negative $\Delta^{33}S$ signatures. Indeed, hydrothermally-influenced Archaean deposits tend to exhibit negative $\Delta^{33}S$ (refs 24–28). Subduction of hydrothermally-altered Archaean basalt into the mantle can produce a negative $\Delta^{33}S$ reservoir of subducted oceanic lithosphere in the deep mantle that may also help to explain the apparent bias to positive $\Delta^{33}S$ values seen in compilations of published analyses[6,7]. Therefore, the negative $\Delta^{33}S$ of sulphides analysed here point to an ancient crustal source with oceanic affinities for Mangaia sulphur. An origin associated with Archaean crustal material is also consistent with other geochemical characteristics of the Mangaia lavas, such as the radiogenic Pb-isotope compositions[1,3,4,10].

The S-isotope compositions from Mangaia require a protolith with the unusual combination of negative $\Delta^{33}S$ and negative $\delta^{34}S$ values. Whereas the negative $\Delta^{33}S$ can only have been generated in the Archaean atmosphere, the origin of the negative $\delta^{34}S$ signature in Mangaia sulphides is less well-constrained. Archaean volcanogenic massive sulphide (VMS) deposits hosted in komatiites represent a possible candidate for the recycled protolith melted beneath Mangaia, as such deposits can have both the negative $\Delta^{33}S$ and negative $\delta^{34}S$ (ref. 24) that approach those identified in Mangaia sulphides. Komatiites may have been commonly erupted on the seafloor during the Archaean[29], where they could have incorporated negative $\Delta^{33}S$ values by seawater sulphate reduction at hydrothermal settings, as evidenced by some Archaean VMS deposits[24]. Therefore, one possible model for the S-isotope composition of Mangaia sulphides is that it originates in hydrothermally-modified mafic sources, similar to the komatiite-hosted VMS deposits[24], that were subsequently subducted into the mantle during the Archaean.

Whereas VMS deposits trend in the direction of negative $\Delta^{33}S$ and negative $\delta^{34}S$ identified in Mangaia sulphides, the available S-isotope data on VMS deposits do not extend to the low $\delta^{34}S$ values we observe in Mangaia. Therefore, we cannot exclude alternative mechanisms that might have generated the combination of negative $\Delta^{33}S$ and negative $\delta^{34}S$ in the Archaean. The combination of negative $\Delta^{33}S$ and $\delta^{34}S$ (down to −0.71‰ and −8.3‰, respectively) was identified in Archaean sulphides from the Gamohaan formation, South Africa[30], where negative $\delta^{34}S$ was attributed to bacterial reduction of sulphate (a process demonstrated to generate extreme negative $\delta^{34}S$ signatures[31]) while preserving its negative $\Delta^{33}S$ anomaly inherited from photolytic reactions in the atmosphere. High degrees of melt degassing under reducing conditions might also generate highly negative $\delta^{34}S$ values, but this would require the melt to have initially negative $\Delta^{33}S$, inherited from the Archaean atmosphere, so that the final degassed product has the combination of S-isotope compositions observed in Mangaia inclusions. Although the exact mechanism for generating negative $\delta^{34}S$ is unknown, the key feature in the Mangaia data set is that the sulphide inclusions and bulk olivine separate have $\Delta^{33}S$ anomalies that could only have been generated in the Archaean atmosphere.

The identification of MIF S in Mangaia lavas places two critical constraints on the origin of the HIMU mantle. First, several recent models invoke metasomatic processes occurring within the mantle to generate the HIMU reservoir (see, for example, refs 12 and 13), but such models do not explicitly invoke materials recycled from surface reservoirs and therefore cannot explain MIF S in HIMU lavas. The discovery of MIF S requires subduction of surface materials into the mantle to generate the HIMU reservoir sampled by Mangaia lavas. Second, the $\Delta^{33}S$ anomaly associated with Mangaia lavas places a lower limit on the formation age of the HIMU mantle domain, namely, 2.45 Gyr ago (Supplementary Fig. 2). The Archaean age for HIMU formation indicated by S isotopes conflicts with earlier estimates that are based on two-stage Pb-isotope model ages of ~1.8 Gyr ago (ref. 10), and this discrepancy may imply a more complicated history for Pb isotopes (that is, more than two stages of Pb differentiation are possible) than generally assumed for the generation of the HIMU mantle. The >2.45-Gyr age constraint from S isotopes indicates that mantle heterogeneities generated by subduction of surface materials into the mantle can be preserved over long timescales—from the Archaean to present—in the convecting mantle.

The new $\Delta^{33}S$ measurements confirm inferences about the cycling of sulphur between the major reservoirs from the Archaean to the Phanerozoic, extending from the atmosphere and oceans to the crust and mantle, and ultimately through a return cycle to the surface that, here, is completed in Mangaia lavas. It remains to be seen whether lavas erupted at other HIMU hotspots and hotspots sampling different

compositional mantle endmembers (for example, EM1 and EM2) will exhibit evidence for recycling of Archaean protoliths.

METHODS SUMMARY

Three basaltic rock samples from Mangaia were crushed, sieved and picked for olivines hosting melt inclusions. Two of the four sulphides analysed here were homogenized using two different techniques (see Methods), and the other two sulphides were not homogenized. Following exposure of the sulphides, the samples were pressed in indium, dried in a furnace, cleaned and then gold coated for SIMS analyses.

In situ Pb- and S-isotope measurements were made using a CAMECA IMS 1280 SIMS instrument at the Swedish Museum of Natural History, Stockholm (NordSIMS facility). All four isotopes of Pb were measured at a mass resolution of 4,860 ($M/\Delta M$) by static four-electron multiplier configuration using a $^{16}O_2^-$ primary ion beam with 23 kV incident energy. Corrections for instrumental mass fractionation were made using natural basaltic glass standards.

The three most abundant S-isotopes (^{32}S, ^{33}S and ^{34}S) were measured at a mass resolution of 4,860 ($M/\Delta M$; sufficient to resolve $^{33}S^-$ from $^{32}S^1H^-$) by static multicollection on Faraday detectors using a $^{133}Cs^+$ primary beam with an incident energy of 20 kV. Corrections for instrumental mass fractionation were made using natural sulphide standards. Full procedures for Pb- and S-isotope analysis at NordSIMS are outlined in the Methods.

Sulphur isotope measurements were made on sulphide inclusions in acid-washed olivine separates from sample MGA-B-47. Sulphur was extracted using Cr reduction techniques and converted to silver sulphide that was analysed as SF_6 by gas-source IRMS at the University of Maryland using techniques described in the Methods.

Major element compositions of sulphides, host-olivine and glass were determined using a CAMECA SX100 electron microprobe at the Laboratoire Magmas et Volcans, Clermont-Ferrand, France.

Full Methods and any associated references are available in the online version of the paper.

Received 16 October 2012; accepted 14 February 2013.

1. Hofmann, A. W. & White, W. M. Mantle plumes from ancient oceanic crust. *Earth Planet. Sci. Lett.* **57,** 421–436 (1982).
2. White, W. & Hofmann, A. Sr and Nd isotope geochemistry of oceanic basalts and mantle evolution. *Nature* **296,** 821–825 (1982).
3. Hauri, E. & Hart, S. R. Re-Os isotope systematics of HIMU and EMII oceanic island basalts from the south Pacific Ocean. *Earth Planet. Sci. Lett.* **114,** 353–371 (1993).
4. Hanyu, T. *et al.* Geochemical characteristics and origin of the HIMU reservoir: a possible mantle plume source in the lower mantle. *Geochem. Geophys. Geosyst.* **12,** Q0AC09, http://dx.doi.org/10.1029/2010GC003252 (2011).
5. Farquhar, J., Bao, H. & Thiemens, M. Atmospheric influence of Earth's earliest sulfur cycle. *Science* **289,** 756–758 (2000).
6. Farquhar, J., Zerkle, A. L. & Bekker, A. Geological constraints on the origin of oxygenic photosynthesis. *Photosynth. Res.* **107,** 11–36 (2011).
7. Johnston, D. T. Multiple sulfur isotopes and the evolution of Earth's surface sulfur cycle. *Earth Sci. Rev.* **106,** 161–183 (2011).
8. Farquhar, J., Wing, B., McKeegan, K. & Harris, J. Mass-independent sulfur of inclusions in diamond and sulfur recycling on early Earth. *Science* **298,** 2369–2372 (2002).
9. Thomassot, E. *et al.* Metasomatic diamond growth: a multi-isotope study (^{13}C, ^{15}N, ^{33}S, ^{34}S) of sulphide inclusions and their host diamonds from Jwaneng (Botswana). *Earth Planet. Sci. Lett.* **282,** 79–90 (2009).
10. Zindler, A. & Hart, S. Chemical geodynamics. *Annu. Rev. Earth Planet. Sci.* **14,** 493–571 (1986).
11. Kelley, K. A., Plank, T., Farr, L., Ludden, J. & Staudigel, H. Subduction cycling of U, Th, and Pb. *Earth Planet. Sci. Lett.* **234,** 369–383 (2005).
12. Niu, Y. & O'Hara, M. J. Origin of ocean island basalts: a new perspective from petrology, geochemistry, and mineral physics considerations. *J. Geophys. Res.* **108,** 2209–2228 (2003).
13. Pilet, S., Baker, M. B. & Stolper, E. M. Metasomatized lithosphere and the origin of alkaline lavas. *Science* **320,** 916–919 (2008).
14. Turner, D. & Jarrard, R. K-Ar dating of the Cook-Austral island chain: a test of the hot-spot hypothesis. *J. Volcanol. Geotherm. Res.* **12,** 187–220 (1982).
15. Chaussidon, M., Albarède, F. & Sheppard, S. M. F. Sulphur isotope variations in the mantle from ion microprobe analyses of micro-sulphide inclusions. *Earth Planet. Sci. Lett.* **92,** 144–156 (1989).
16. Saal, A. E., Hart, S. R., Shimizu, N., Hauri, E. H. & Layne, G. D. Pb isotopic variability in melt inclusions from oceanic island basalts, Polynesia. *Science* **282,** 1481–1484 (1998).
17. Yurimoto, H. *et al.* Lead isotopic compositions in olivine-hosted melt inclusions from HIMU basalts and possible link to sulfide components. *Phys. Earth Planet. Inter.* **146,** 231–242 (2004).
18. Ono, S., Wing, B., Johnston, D., Farquhar, J. & Rumble, D. Mass-dependent fractionation of quadruple stable sulfur isotope system as a new tracer of sulfur biogeochemical cycles. *Geochim. Cosmochim. Acta* **70,** 2238–2252 (2006).
19. Shen, Y. *et al.* Multiple S-isotopic evidence for episodic shoaling of anoxic water during Late Permian mass extinction. *Nature Commun.* **2,** 210 (2011).
20. Rouxel, O., Ono, S., Alt, J., Rumble, D. & Ludden, J. Sulfur isotope evidence for microbial sulfate reduction in altered oceanic basalts at ODP Site 801. *Earth Planet. Sci. Lett.* **268,** 110–123 (2008).
21. Taylor, B. The single largest oceanic plateau: Ontong Java-Manihiki-Hikurangi. *Earth Planet. Sci. Lett.* **241,** 372–380 (2006).
22. Frey, F. *et al.* Origin and evolution of a submarine large igneous province: the Kerguelen Plateau and Broken Ridge, southern Indian Ocean. *Earth Planet. Sci. Lett.* **176,** 73–89 (2000).
23. Kamenetsky, V., Maas, R. & Sushchevskaya, N. Remnants of Gondwanan continental lithosphere in oceanic upper mantle: evidence from the South Atlantic Ridge. *Geology* **29,** 243–246 (2001).
24. Bekker, A. *et al.* Atmospheric sulfur in Archean komatiite-hosted nickel deposits. *Science* **326,** 1086–1089 (2009).
25. Farquhar, J. & Wing, B. in *Mineral Deposits and Earth Evolution* (eds McDonald, I., Boyce, A. J., Butler, I. B., Herrington, R. J. & Polya, D. A.) 167–177 (Spec. Publ. 248, Geol. Soc. Lond., 2005).
26. Ueno, Y., Ono, S., Rumble, D. & Maruyama, S. Quadruple sulfur isotope analysis of ca. 3.5 Ga Dresser Formation: new evidence for microbial sulfate reduction in the early Archean. *Geochim. Cosmochim. Acta* **72,** 5675–5691 (2008).
27. Bao, H., Rumble, D. & Lowe, D. R. The five stable isotope compositions of Fig Tree barites: implications on sulfur cycle in ca. 3.2Ga oceans. *Geochim. Cosmochim. Acta* **71,** 4868–4879 (2007).
28. Jamieson, J., Wing, B., Hannington, M. & Farquhar, J. Evaluating isotopic equilibrium among sulfide mineral pairs in Archean ore deposits: case study from the Kidd Creek VMS deposit, Ontario, Canada. *Econ. Geol.* **101,** 1055–1061 (2006).
29. Grove, T. L. & Parman, S. W. Thermal evolution of the Earth as recorded by komatiites. *Earth Planet. Sci. Lett.* **219,** 173–187 (2004).
30. Kamber, B. S. & Whitehouse, M. J. Micro-scale sulphur isotope evidence for sulphur cycling in the late Archean shallow ocean. *Geobiology* **5,** 5–17 (2007).
31. McLoughlin, N., Grosch, E. G., Kilburn, M. R. & Wacey, D. Sulfur isotope evidence for a Paleoarchean subseafloor biosphere, Barberton, South Africa. *Geology* **40,** 1031–1034 (2012).

Supplementary Information is available in the online version of the paper.

Acknowledgements M.G.J. acknowledges Boston University start-up funds and NSF grant EAR-1145202 that supported this work. E.F.R.-K. and K.T.K. acknowledge support from EU SYNTHESYS and French ANR SlabFlux, this is Laboratory of Excellence *ClerVolc* contribution number 54. The NordSIMS facility is financed and operated under a joint Nordic contract; this is NordSIMS contribution number 337. We thank B. White for his review of the manuscript, and P. Cartigny and J. Labidi for discussion. We thank D.T. Johnston, D. Papineau, O. J. Rouxel and S. Ono for advice in compiling the global S-isotope database. We also thank N. Shimizu, B. D. Monteleone, E. A. Price, and P. Schiano for assistance with sample preparation.

Author Contributions R.A.C. wrote the paper and prepared the figures and tables. M.G.J. conceived the project. R.A.C., E.F.R.-K, K.T.K. and M.G.J. performed sample preparation. M.J.W. performed the *in situ* SIMS analyses. J.F. and M.A.A. performed the S-isotope analyses on bulk olivine separates. J.M.D.D. and E.H.H. aided in the field. All authors participated in the discussion and interpretation of results, and preparation of the manuscript.

Author Information Reprints and permissions information is available at www.nature.com/reprints. The authors declare no competing financial interests. Readers are welcome to comment on the online version of the paper. Correspondence and requests for materials should be addressed to R.A.C. (racabral@bu.edu).

METHODS

Sample preparation and selection. Three basaltic samples (MG1001, MGA-B-25 and MGA-B-47) were crushed and sieved. Olivines hosting melt inclusions were picked using a binocular microscope. One olivine-hosted melt inclusion (sample MGA-B-47) was homogenized using a Vernadsky-type heating stage while monitoring the homogenization temperature of the inclusion. Batches of 50–150 mg of olivine crystals from sample MG-1001 were homogenized using a gas-mixing furnace at 1,280 °C for 20 min at a near iron–wüstite buffer condition. Duration and oxygen fugacity of this batch homogenization technique closely mimicked the homogenization procedure by the heating stage. Two sulphide inclusions were homogenized, but the other two (MGA-B-25 and MG1001-S14) were not. Following exposure of the sulphides by polishing, sulphides were pressed into an indium mount, re-polished, cleaned with deionized water, and dried at 100 °C for 24 h before applying a gold coat.

***In situ* lead isotope measurements.** *In situ* Pb-isotope measurements of the sulphides used methods described elsewhere[32]. A −13 kV $^{16}O_2^-$ primary ion beam illuminated a 200 μm mass aperture to produce a ~7–8 nA, 20 μm, slightly elliptical, flat bottomed crater. Target areas were subjected to a 180 s pre-sputter with a 25 × 25 μm raster to remove the Au coating and clean the surface of extraneous Pb. The unrastered 10 kV secondary ion beam was centred in a 4,000 μm field aperture (field of view on the sample approximately 25 × 25 μm at 160× transfer magnification) by scanning the transfer deflectors, and the beam was maximized to the peak of the energy distribution (45 eV window) by scanning the sample voltage. The magnetic field was locked at high precision using an NMR field sensor throughout the analytical session. The mass spectrometer used an entrance slit width of 60 μm and a common exit slit width of 250 μm on four ion counting secondary electron multipliers (EMs), corresponding to a mass resolution ($M/\Delta M$) of 4860, sufficient to resolve Pb from molecular interferences in sulphides and glasses. The detectors were positioned for simultaneous detection of ^{204}Pb, ^{206}Pb, ^{207}Pb and ^{208}Pb. Measurements consisted of 40–120 cycles of 20 s integration. An electronically gated 60 ns deadtime correction was used. Typical background levels on the EMs were <0.02 c.p.s., which was negligible at the level of Pb signal measured. Each set of 40 cycles took ~20 min. See Supplementary Information for discussion of internal and external precision for *in situ* analyses of Pb isotopes.

***In situ* sulphur-isotope measurements.** Multiple S-isotope measurements followed the analytical protocol described by ref. 33. A −10 kV primary beam of $^{133}Cs^+$ was critically focused onto the sample, yielding a 2 nA primary beam and spot with a diameter of ~5 μm which was rastered over 5 × 5 μm during data acquisition to homogenize the sampling. Target areas were subjected to a 70 s pre-sputter with a 20 × 20 μm raster to remove the Au coating. The 5 × 5 μm rastered 10 kV secondary ion beam was centred in a 2,500 μm field aperture (field of view on the sample of ~25 × 25 μm at 100× transfer magnification) by automated scanning of the transfer deflectors. Sample charging was minimized by use of a low-energy normal-incidence electron gun and no energy adjustments were necessary. The magnetic field was locked at high precision using an NMR field sensor for the entire analytical session. The mass spectrometer used an entrance slit width of 90 μm and a common exit slit width of 250 μm on the three Faraday detectors used to measure ^{32}S, ^{33}S and ^{34}S, corresponding to a mass resolution ($M/\Delta M$) of 4,860. Faraday amplifiers were housed in an evacuated, thermally stabilized chamber and used a 10^{10} Ω input resistor on the ^{32}S channel and 10^{11} Ω on the other channels. Typical secondary ion signals of 10^9 c.p.s. on ^{32}S were obtained and each analysis consisted of 64 s of data integration.

The S-isotope data were obtained in two analytical sessions. Analyses of the unknown sulphides were bracketed by measurements of two non-MIF pyrite standards, Ruttan and Balmat[34] and a MIF pyrite from the Isua Greenstone Belt[33]. Ruttan alone was used for calculation of instrumental mass fractionation while Ruttan, Balmat and the Isua pyrite were used to constrain the mass dependent fractionation line for each session. In the second session, an in-house, strongly negative δ^{34}S pyrite concretion (Gabon) was used to further verify the mass dependent fractionation line, but was not used to calculate instrumental mass fractionation or to constrain the mass dependent fractionation line. See Supplementary Information for external precision of S-isotope measurements.

Sulphur-isotope measurements on bulk olivines. Sulphur isotope measurement of sulphide inclusions in ~400 mg of olivine separates from sample MGA-B-47 were extracted using chemical techniques and measured by gas source isotope ratio mass spectrometry at the University of Maryland. Acid washed (HF and HCl) olivine separates were crushed in an agate mortar under ethanol and transferred to an apparatus like that described in ref. 35 where they were reacted with a hot acidic Cr(II) solution. Sulphide released in this process was captured as silver sulphide, which was washed, dried and wrapped in clean Al foil. The foil with silver sulphide was placed in a Ni tube where it was reacted with fluorine gas, overnight at 250 °C. Product SF_6 was purified using cryogenic and chromatographic techniques, and frozen into a micro inlet on a ThermoFinnigan MAT 253, which was used for determination of isotope ratios. The sample size was small (100 μg) and the fluorination yield was low (50%), suggesting either adsorbed water on the Al foil or possible contaminants (for example, Al oxide coatings and oils that may not have been completely cleaned off of the foil) in the silver sulphide. Uncertainties for Δ^{33}S are inferred from the mass spectrometry analyses, which yielded ±0.04‰ (2σ). Uncertainties for δ^{34}S are estimated to be larger (±1‰, 2σ) due to contributions of mass dependent fractionation during the chemical preparation (extraction, conversion and purification) of sulphur or mass spectrometric analysis. The long-term reproducibility on fluorination is 0.016 (2σ s.d.) for Δ^{33}S and 0.30 (2σ s.d.) for δ^{34}S. Short-term reproducibility can be better for δ^{34}S and in rare cases for Δ^{33}S.

Major element measurements. Electron microprobe analysis for the determination of major element concentrations was completed at the Laboratoire Magmas et Volcans, Clermont-Ferrand, France, on a Cameca SX 100 using standard procedures.

32. Rose-Koga, E. F. *et al.* Mantle source heterogeneity for South Tyrrhenian magmas revealed by Pb isotopes and halogen contents of olivine-hosted melt inclusions. *Chem. Geol.* **334,** 266–279 (2012).
33. Whitehouse, M. J. Multiple sulfur isotope determination by SIMS: evaluation of reference sulfides for Δ^{33}S with observations and a case study on the determination of Δ^{36}S. *Geostand. Geoanal. Res.* http://dx.doi.org/10.1111/j.1751-908X.2012.00188.x (published online 7 January 2013).
34. Crowe, D. E. & Vaughan, R. G. Characterization and use of isotopically homogeneous standards for in situ laser microprobe analysis of ^{34}S/^{32}S ratios. *Am. Mineral.* **81,** 187–193 (1996).
35. Forrest, J. & Newman, L. Ag-110 microgram sulphate analysis for short time resolution of ambient levels of sulphur aerosol. *Anal. Chem.* **49,** 1579–1584 (1977).